Society For Biomaterials

Polyelectrolyte membrane scaffold sustains growth of neuronal cells

A. Grzeczkowicz,[1†] J. Gruszczynska-Biegala,[2†] M. Czeredys,[2] A. Kwiatkowska,[1] M. Strawski,[3] M. Szklarczyk,[3] M. Koźbiał,[4] J. Kuźnicki,[2] L. H. Granicka[1]

[1]Nalecz Institute of Biocybernetics and Biomedical Engineering Polish Academy of Sciences, Warsaw, Poland
[2]International Institute of Molecular and Cell Biology in Warsaw, Warsaw, Poland
[3]Laboratory of Electrochemistry Faculty of Chemistry University of Warsaw, Warsaw, Poland
[4]Institute of Physical Chemistry Polish Academy of Sciences, Warsaw, Poland

Received 28 November 2018; accepted 18 December 2018
Published online 4 February 2019 in Wiley Online Library (wileyonlinelibrary.com). DOI: 10.1002/jbm.a.36599

Abstract: Cell immobilization within nano-thin polymeric shells can provide an optimal concentration of biological material in a defined space and facilitate its directional growth. Herein, polyelectrolyte membrane scaffolds were constructed using a layer-by-layer approach to determine the possibility of promoting improved growth of rat cortical neuronal cells. Membrane presence was confirmed by Fourier transform infrared spectroscopy, Zeta potential, and atomic force and scanning electron microscopy. Scaffold performance toward neuronal cell growth was assessed in vitro during a 14-day culture. Cell conditions were analyzed immunocytochemically. Furthermore, western blot and real-time PCR analyses were used to validate the presence of neuronal and glial cells on the scaffolds. We observed that alginate/chitosan, alginate/polylysine, and polyethyleneimine/chitosan scaffolds promote neuronal growth similarly to the control, poly-D-lysine/laminin. We conclude that membranes maintaining cell viability, integrity and immobilization in systems supporting neuronal regeneration can be applied in neurological disease or wound healing treatment. © 2018 The Authors. *Journal of Biomedical Materials Research Part A* published by Wiley Periodicals, Inc. J Biomed Mater Res Part A: 107A: 839–850, 2019.

Key Words: immobilization, polyelectrolyte, neuronal and glial cells, layer-by-layer, adhesion

How to cite this article: Grzeczkowicz A, Gruszczynska-Biegala J, Czeredys M, Kwiatkowska A, Strawski M, Szklarczyk M, Koźbiał M, Kuźnicki J, Granicka LH. 2019. Polyelectrolyte membrane scaffold sustains growth of neuronal cells. J Biomed Mater Res Part A 2019:107A:839–850.

INTRODUCTION

The application of nanotechnology to neuroscience has many advantages, including understanding the functional structure of cognition and information processing. Fundamental issues to consider in neuronal engineering are neuron functionality, neurite outgrowth, and synaptic function. Other pertinent questions include cell viability on fabricated surfaces as well as long-term stability and retention of biological function. Dissociated cells from any central nervous system region contained neurons, astrocytes, oligodendrocytes, and other glial cells.[1,2] In contrast to glial cells, which easily adhere to many untreated surfaces, neurons are remarkably sensitive to the nature of the substrate and require specific surfaces for adhesion. The search for an optimum surface for exogenous primary neuronal cell growth is under intense investigation, including evaluating polyelectrolyte (PE) membranes as substrates for neuronal cell growth.[3–5] One type of membrane is made of graphene and its derivatives; its effect on the behavior and differentiation of neuronal and stem cells was previously described.[6,7] The PEs used to form the layers may contain not only ionizable electrolyte groups, but also additional functionality imparted by the polymer structure.[8–13] For instance, hydroxylated fullerene incorporated into layers may increase hydrophilicity and improve layer stability.[14]

A membrane scaffold can be constructed with PE multilayers by applying the layer-by-layer (LbL) technique, using polymer self-assembly processes to form the PE multilayers. PE multilayer formation can be driven by different processes, including electrostatic interactions between oppositely charged constituents,[15] hydrogen bonding,[14,16–18] covalent bonding,[19] and hydrophobic interactions.[19,20] Different materials of proven biocompatibility and/or biodegradability are typically used to form membrane layers of a scaffold. Among them the following ones can be enumerated: polyethyleneimine, alginate, polylysine, and chitosan, which are described further below.

Chitosan is a widely-used cationic linear co-polymer of β(1-4)-linked D-glucosamine, generated *via* chitin *N*-deacetylation.[21] It is extracted from the skeletal materials of

†These authors contributed equally to this work.
Correspondence to: L. H. Granicka; e-mail: lgranicka@ibib.waw.pl
Contract grant sponsor: National Science Centre in Poland; contract grant number: DEC-2011/01/D/NZ3/02051 and 2014/15/D/NZ3/05181

the crustacean cuticles of arthropods (shrimps, insects, and crabs) and from the cell walls of miscellaneous fungi. This biocompatible and biodegradable PE has a positive charge and a high degree of chemical reactivity due to numerous free amino groups in its chemical structure. Moreover, chitosan exhibits excellent biological and physicochemical properties for use in neuronal regeneration.[21]

Alginate is a water soluble, natural copolymer of α-L-guluronic acid and β-D-mannuronic acid units.[22] Anionic polysaccharide is obtained from many different species of brown algae. Due to its simple gelation with divalent cations, such as Ca^{2+}, it is commonly employed for living cell encapsulation.[23] In the presence of polycations like poly-L-lysine or chitosan, alginate can form PE complexes.

Polylysine as poly-L-lysine is a positively charged immunogenic amino acid polymer. It is also reported to attract host inflammatory cells.[24] Poly-L-lysine may be a useful attachment factor for cells by promoting cell adhesion to solid substrates by enhancing electrostatic interactions between negatively charged ions in the cell membrane and culture surface. Moreover, the synthetic PE-polyethyleneimine cationic, highly protonable synthetic polymer was employed in this study, which is commonly used to culture weakly anchoring cells to increase attachment. Polyethyleneimine is also established as an efficient transfection reagent.[25]

Due to their nontoxicity, degradability and biological compatibility, as a membrane constituents we employed two natural PEs: chitosan and sodium alginate. In the present study, we fabricated a system for neuronal cell growth using an LbL technique that involves the sequential deposition of oppositely charged PEs to build up nano-thin multilayers to construct scaffolds for cell immobilization.

The performance of the PE scaffolds in different conformations was analyzed *in vitro* to assess the usability of evaluated membranes in the directional cell growth of immobilized neuronal cells. Furthermore, the morphology of the system of neurons immobilized within the constructed scaffolds was evaluated using scanning electron microscopy.

The presence of membrane layers was examined using Fourier-transform infrared spectroscopy (FTIR) and atomic force microscopy (AFM) techniques. The influence of scaffold layer conformation on multilayer assembly was assessed by evaluating intralayer adhesion of the membrane system *via* AFM.

Moreover, the functional structure of neuronal cells immobilized within the evaluated membranes was examined with different dyes and antibodies using fluorescence light microscopy. These results, together with western blot and real-time PCR analyses of cultured rat cortical neurons, showed that the cells growing on all membranes express both neuronal and glial markers.

MATERIALS AND METHODS

Materials

Reagents. Chitosan from crab shells, sodium alginate, polyethyleneimine (MW 60kD), poly-L-lysine hydrobromide (MW15-30kD), hydrated polyhydroxy small gap fullerenes, bovine serum albumin (BSA), 4′,6-diamidino-2-phenylindole (DAPI) nuclear stain and (3-4,5-dimethylthiazol-2-yl)-2,5-diphenyltetrazolium bromide (MTT) were purchased from Sigma-Aldrich (St. Louis, MO, USA). Neurobasal medium, B27 supplement, glutamine, and glutamate were purchased from Life Technologies (Carlsbad, CA, USA). Anti-microtubule-associated protein 2 (MAP2) antibody was purchased from Cell Signaling Technology (Danvers, MA, USA), and anti-glial fibrillary acidic protein (GFAP) antibody was purchased from Sigma-Aldrich (St. Louis, MO, USA).

Multilayer film assembly

The following PEs were used to build multilayer films: chitosan (CHIT), sodium alginate (ALG), polyethyleneimine (PEI), poly-L-lysine (PLL). Solutions of PEI or PLL were prepared at a concentration 1 mg/mL in 0.1 M NaCl; alginate solution was prepared at a concentration 0.5 mg/mL in 0.1 *M* NaCl, and chitosan solution was prepared at concentration 1 mg/mL in 2.5% acetic acid. To obtain the polyethyleneimine (PEI) with fullerenol complex (PEI/FUOL), fullerenol solution in 0.1 *M* NaCl (pH 7.2) at a concentration of 0.5 mg/mL was added to PEI at a 1:10 ratio and subsequently stirred for 4 h at room temperature, as previously described.[14] Multilayer films were prepared on glass coverslips, which served as the solid surface for membrane scaffold positioning. Prior to film deposition, glass coverslips were cleaned with 70% ethanol, rinsed thoroughly with deionized, sterile water and air dried. Coverslips were next sterilized in an autoclave, immersed in sodium alginate, PEI or PEI/FUOL solution for 30 min, and dried. Next, coverslips were dipped in chitosan or PLL solution for 30 min, and dried. The physicochemical properties of six PE membranes were evaluated using potential Zeta measurement, FTIR and AFM: PEI/PLL, PEI + FUOL/PLL, PEI/CHIT, PEI + FUOL/CHIT, ALG/CHIT, and ALG/PLL.

Primary neuronal cell isolation and culture

The following experimental procedures were approved by the Local Commission for the Ethics of Animal Experimentation no. 1 in Warsaw. Cortical neuron cultures were prepared from 19-day-old embryonic (E19) Wistar rat brains as previously described.[26] Brains were removed from rat embryos and collected in cold Hank's solution (Hank's Balanced Salt Solution (HBSS) supplemented with 15 m*M* HEPES buffer and penicillin/streptomycin). The cortex was isolated, rinsed three times in cold Hank's solution, and treated with trypsin for 35 min. The E18 cortex was, upon dissection, immediately dissociated into individual neurons and eventually non-neuronal cells. Primary cortical neurons were plated at a density of $90 \times 10^3/cm^2$. Neurons were grown in Neurobasal medium (Life Technologies, Carlsbad, CA, USA) supplemented with 2% B27 (Life Technologies, Carlsbad, CA, USA), 0.5 m*M* glutamine (Invitrogen, Carlsbad, CA, USA), 12.5 μ*M* glutamate (Invitrogen), and a penicillin (100 U/mL)/streptomycin mixture (100 mg/mL). Cultures were maintained at 37°C in a humidified 5% CO_2/95% atmosphere.

The immobilized cell culture

Neuronal cells immobilized within scaffolds were incubated (5% CO_2, 37°C) in Neurobasal medium for 6 days, and then

half of the medium was changed every 3 days with Neurobasal medium supplemented with B27, 0.5 m*M* glutamine and a penicillin/streptomycin mixture. As a negative control, neuronal cells positioned on a glass support were cultured (5% CO_2, 37°C) for 2 weeks. Immobilized cells were examined after 24 h, 48 h, and 2 weeks of culture *via* fluorescence microscopy using a Nikon Eclipse 80i. Scanning electron microscopy (SEM) using a Hitachi TM-1000 was used to evaluate system morphology.

AFM evaluation

A Nanoscope V AFM microscope (Veeco Instruments, Inc., Plainview, NY, USA) was used to image sample surfaces. Surface morphology in non-contact mode was imaged. PE layers were visualized in 2D/3D form using dedicated software (Nanoscope 7.30). Images were obtained at room temperature.

For surface forces acquisition a silicon cantilever with a borosilicate glass colloidal particle sphere with a 10 μm diameter (SQube) was applied. The spring constant value of the cantilever was determined before each experiment using the Thermal Tune method. Force–distant curves were acquired with dedicated Nanoscope 7.30 software and analyzed with Origin 8.50 (OriginLab, Northampton, MA, USA). Forces were measured 5 s after interaction. The maximum load force was set to 20 n*N*. The work of adhesion was calculated by integrating force distance dependencies according to the formula

$$W_{\mathrm{ad}} = \int F_{\mathrm{ad}}\, dz,$$

where F_{ad} is adhesion force and z is the distance of the sphere from a surface. All adhesion measurements were carried out under in situ conditions (0.15 *M* NaCl). PE pH in deposition solution was 7.0.

Zeta potential evaluation

Zeta potential evaluation was performed in a Zeta Potential Analyzer Zetasizer Nano Z (Malvern Instruments, Malvern, UK) using the following parameters: electrical field, 8–10 V/cm; measure time, 20–120 s; temperature measure, 20°C; and conductivity, 120–150 mS/cm.

FTIR measurements

Evaluation of spectrum of absorption for red irradiation (FTIR) was performed using an FTS 3000MX (Bio Rad Excalibur, Hercules, CA, USA) device. FTIR curves were analyzed using Essential FTIR software. The presence of PE layers on the substrate was assessed by evaluating the spectrum of absorption for red irradiation (4000–666 cm^{-1}) before culture. Liquid samples were contained in a KBr pellet, and 30 scans were typically performed at a resolution of 4 cm^{-1} and selectivity of 2 cm^{-1}.

Immunocytochemistry and immunostaining

To visualize cells within the scaffolds, different dyes and antibodies that can distinguish neurons and astrocytes were applied. To identify neurons, cultures were stained with anti-microtubule-associated protein 2 (MAP2), which identifies proteins of the neuronal skeleton, and glial cells were identified using anti-glial fibrillary acidic protein (GFAP). Cells cultured for 14 days were fixed in ice-cold 4% paraformaldehyde and 4% sucrose for 15 min, washed in PBS, permeabilized in 0.1% Triton-X 100 for 10 min before additional washing in PBS. Nonspecific antibody binding was prevented by blocking all samples with 2% normal donkey serum (NDS) for 30 min. After blocking, samples were incubated with primary rabbit antibody against MAP2 (1:500) and mouse antibody against GFAP (1:500) at room temperature for 2 h. Cells were then incubated for 1 h with anti-rabbit Alexa Fluor 488- and anti-mouse Alexa Fluor 594-conjugated antibodies (1:500). To visualize cell nuclei, we included Hoechst 33258 dye (Invitrogen, Carlsbad, CA, USA) in the wash for 5 min after secondary antibody incubation. Coverslips were mounted on slides with ProLong® Gold Antifade Mountant (Life Technologies, Carlsbad, CA, USA). Cells were examined using a fluorescence microscope (Nikon, Tokyo, Japan).

Western blot analysis

For western blot analysis, cells were lysed in RIPA lysis buffer (50 m*M* Tris pH 7.5, 150 m*M* NaCl, 1% NP-40, 0.5% NaDOC, 0.1% SDS, 1 m*M* EDTA, protease inhibitors (Roche, Basel, Switzerland) and phosphatase inhibitors (Sigma-Aldrich, Carlsbad, CA, USA)), then cleared by centrifugation at 12,000*g* for 10 min as previously described.[27] Protein extracts were separated on a 10% SDS-PAGE gel and transferred to a Protran nitrocellulose membrane (GE Healthcare, Little Chalfont, UK). Unoccupied sites on the nitrocellulose membrane were blocked with a 5% solution of non-fat milk in TBS containing 0.1% Tween-20. The nitrocellulose membrane was then incubated with primary antibody (rabbit anti-MAP2, mouse anti-GFAP, or rabbit anti-GAPDH) overnight at 4°C followed by incubation with the suitable secondary antibody conjugated to horseradish peroxidase (HRP). Band intensity was measured using GS-800 Calibrated Densitometer and Quantity One software (Bio Rad, Hercules, CA, USA).

Gene expression analysis by qRT-PCR

Single analyses of gene expression levels in primary cultures of rat cortical neurons cultured on PE scaffolds were performed in individual qRT-PCR reactions using a LightCycler® 96 SW 1.1 system (Roche, Basil, Switzerland). For each reaction, 4 ng of cDNA was used. The obtained data were analyzed using the relative quantification method and $2^{-\Delta\Delta CT}$ formula ($\Delta\Delta CT = \Delta CT_{\mathrm{target}} - \Delta CT_{\mathrm{Gapdh}}$, in which CT is the cycle threshold). Expression of the *Rbfox3/NeuN, Map2, Eno2, Calb2*, *Gfap, S100b* genes was verified using FAM dye-labeled TaqMan probes (Life Technologies, Carlsbad, CA, USA) and TaqMan chemistry (Life Technologies, Carlsbad, CA, USA) as previously described.[28]

Western blot and qRT-PCR experiments were repeated at least three times. Statistical analysis was performed using Prism version 5.02 software (Graph-Pad, San Diego, CA, USA). Data are expressed as the mean ± SD. One-way analysis of variance (ANOVA) was used to analyze sets of western

blot and gene expression data. Tukey's *post hoc* test was used to determine statistically significant differences among groups. The degree of significance vs. the control is indicated by asterisks: *$p < 0.05$, **$p < 0.005$, ***$p < 0.0005$ (ns, not significant; $p > 0.05$).

RESULTS

Nano-thin shell presence was confirmed using AFM and FTIR. AFM visualization of applied PE layers deposited on gold-covered mica substrate is presented in Figure 1(A–E).

Fourier transform infrared spectroscopy spectrum evaluation allowed us to assess PE layer presence on the substrate. For the PE PEI/CHIT configuration, interactions between PEI and CHIT layers can be confirmed by characteristic peak presence at frequency [cm^{-1}] 1277, which represents out-of-plane aromatic C–H vibrations for CHIT; we observed this peak shifted to 1270 due to CHIT interactions with PEI.

For the PEI + FUOL/CHIT configuration, the 1744 peak representing stretching vibrations of the carbonyl group in CHIT shifted to 1717 due to interactions between the PEI + FUOL and CHIT layers.

For the ALG/PLL configuration, the NH stretching vibrations of ALG are normally observed at 1362, but shifted to 1310 due to interactions between the PLL and ALG layers. The spectrum of interactions between PLL/PEI and PLL/PEI + FUOL have been presented elsewhere14. Example FTIR spectrums for membrane ALG, CHIT, and ALG/CHIT are presented in Figure 2.

Layer presence was confirmed by characteristic peaks at the following frequencies [cm^{-1}]: 3278, representing O–H stretching vibrations in ALG, N–H, and O–H stretching vibrations in both CHIT and ALG/CHIT; 1375 representing CH3 vibrations for CHIT led to 1366 vibrations due to interactions between CHIT and ALG; 1277 representing planal aromatic C–H vibrations in CHIT shifted to 1270 due to interactions between CHIT and ALG; 1006 representing the aromatic structure of ALG, CHIT, and ALG/CHIT; 1217 representing vibrations of partially deacetylated CHIT and ALG/CHIT (Fig. 2).

Three types of scaffolds were used for further study, involving PE conformations leading to the following properties:

- A construction with a positively charged potential Zeta in the basal layer, with moderate adhesion between layers (PEI/PLL; PEI + FUOL/PLL).
- A construction with a positively charged potential Zeta in the basal layer, with high adhesion between layers (PEI/CHIT; PEI + FUOL/CHIT).
- A construction with negatively charged potential Zeta in the basal layer (with potential in the layer interfaces close to 0 or of opposite value to that of the basal layer), with low or moderate adhesion between layers (ALG/CHIT; ALG/PLL).

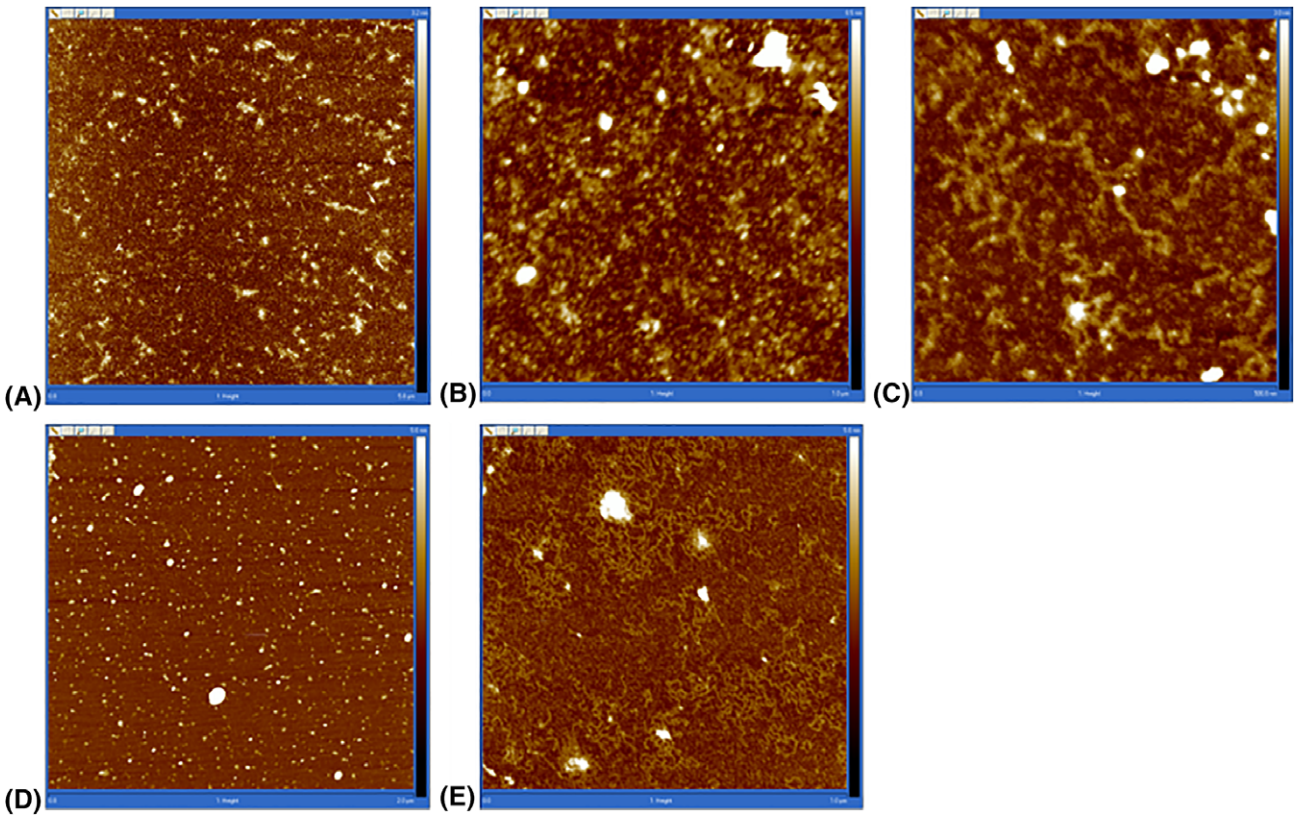

FIGURE 1. AFM visualization of PE layers deposited on gold-covered mica substrate. (A) Polyethyleneimine layer; (B) polyethyleneimine with fullerenol; (C) chitosan layer; (D) polylysine layer; (E) alginate layer.

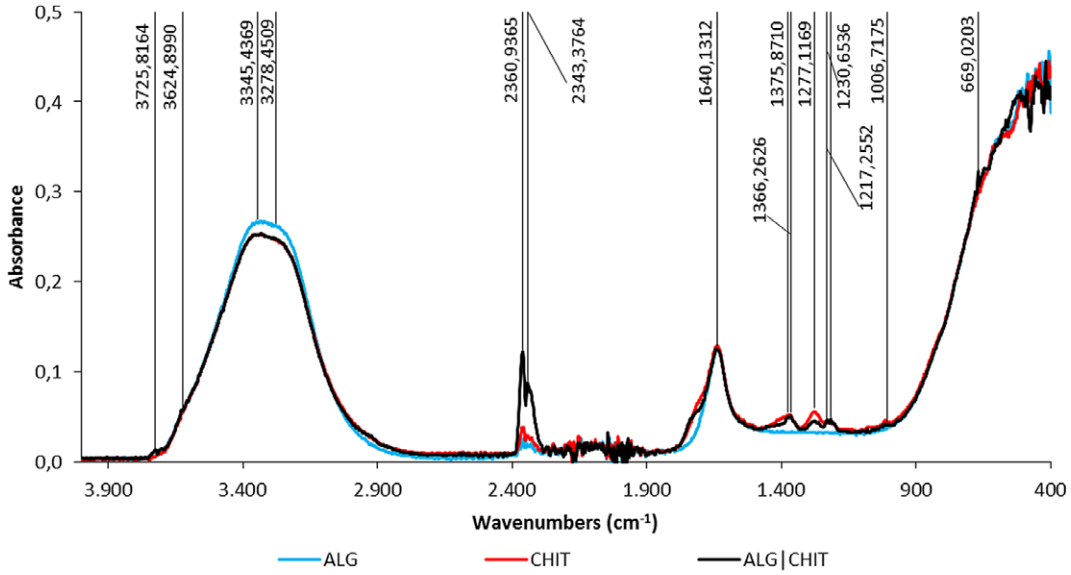

FIGURE 2. Example FTIR spectrums for membrane ALG (blue), CHIT (red), and ALG/CHIT (black).

Evaluation of the membranes

To determine adhesion properties between PE layers combining modified or unmodified PEI or ALG with PLL or CHIT, layers were deposited onto a mica surface and a spherical probe surface. The following systems were applied: mica covered with PEI, PEI + FUOL or ALG and sphere tip covered with PLL or CHIT. The calculated average adhesion work occurring between layers was as follows

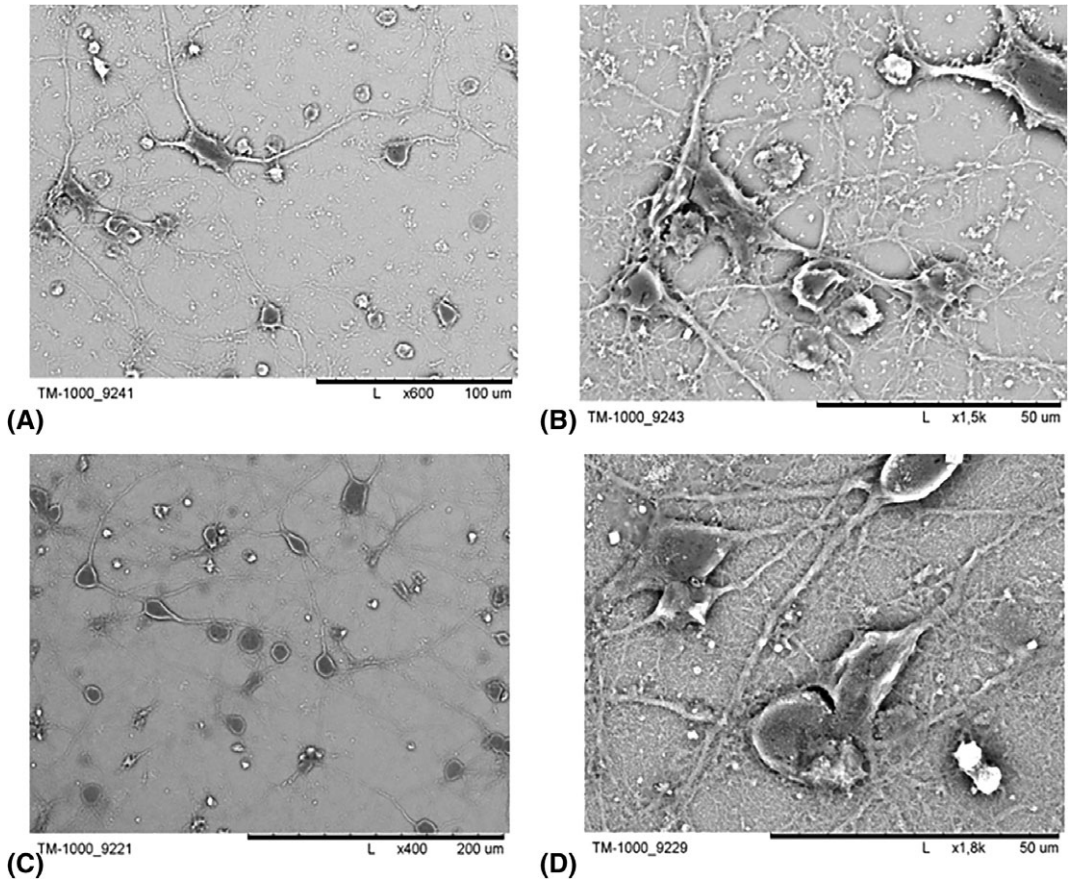

FIGURE 3. Scanning electron microscopy (SEM) pictures of cultured cells immobilized within a polyethyleneimine/polylysine (A, B) or polyethyleneimine with fullerenol/polylysine (C, D) scaffold after 2 weeks of culture. Magnification: (A) ×600; (B) ×1500; (C) ×400; (D) ×1800.

($\times 10^{-17}$ J): PEI/PLL, 19.9 $\pm$ 3.69; PEI + FUOL/PLL, 41.1 $\pm$ 1.95; PEI/CHIT, 174 $\pm$ 4.22; PEI + FUOL/CHIT, 225 $\pm$ 4.80; ALG/CHIT, 0.58 $\pm$ 0.41; and ALG/PLL, 16.5 $\pm$ 8.25. It can be presumed that values less than or equal to 10 are low, from greater than 10 to 100 are moderate, and greater than 100 are high. The potential ZETA [mV] of PEI and ALG was 14.93 $\pm$ 3.07 and -37.60 ± 2.19, respectively.

Design of a membrane with a positively charged potential Zeta in the basal layer, with moderate adhesion between layers

The PEI/PLL construction has been applied as a conformation ensuring suitable conditions for the growth of different cell populations.[29] It is notable that the membrane material PEI/PLL was demonstrated to possess properties blocking bacterial cell transport.[30] The build-up of PEI/PLL multilayers involves mainly hydrogen interactions between layers, thereby building the scaffold with a mildly positive potential in the basal layer (+14.93 $\pm$ 3.07 mV), whereas the external layer does not have an altered potential value (+14.11 $\pm$ 2.36 mV).

The build-up of multilayers involving incorporated fullerenol allowing for increased hydrogen bonding was applied to strengthen the adhesion force between multilayers while retaining mild basal layer potential Zeta changes (about a 17% decline),14 as compared to PEI/PLL.

In both membrane types [Fig. 3(A–D)], we observed cells adhered to the membrane surface.

Design of a membrane with positively charged potential Zeta in the basal layer, with high adhesion between layers

The PEI/CHIT conformation involves mainly electrostatic interactions between layers, and was used to build the scaffold with a mild positive potential in the basal layer (+14.93 $\pm$ 3.07 mV) (Figure 4).

In the PEI/CHIT membrane scaffold, we observed a large increase in biological material, creating a dense layer on the membrane surface. The PEI + FUOL/CHIT conformation involves electrostatic interactions with additional hydrogen bonding between layers as compared to PEI/CHIT, leading to a scaffold with a mildly positive potential in the basal layer (+14.93 $\pm$ 3.07 mV).

The morphology of the PEI + FUOL/CHIT scaffold allows for unusual aggregates of cells adhering to the surface.

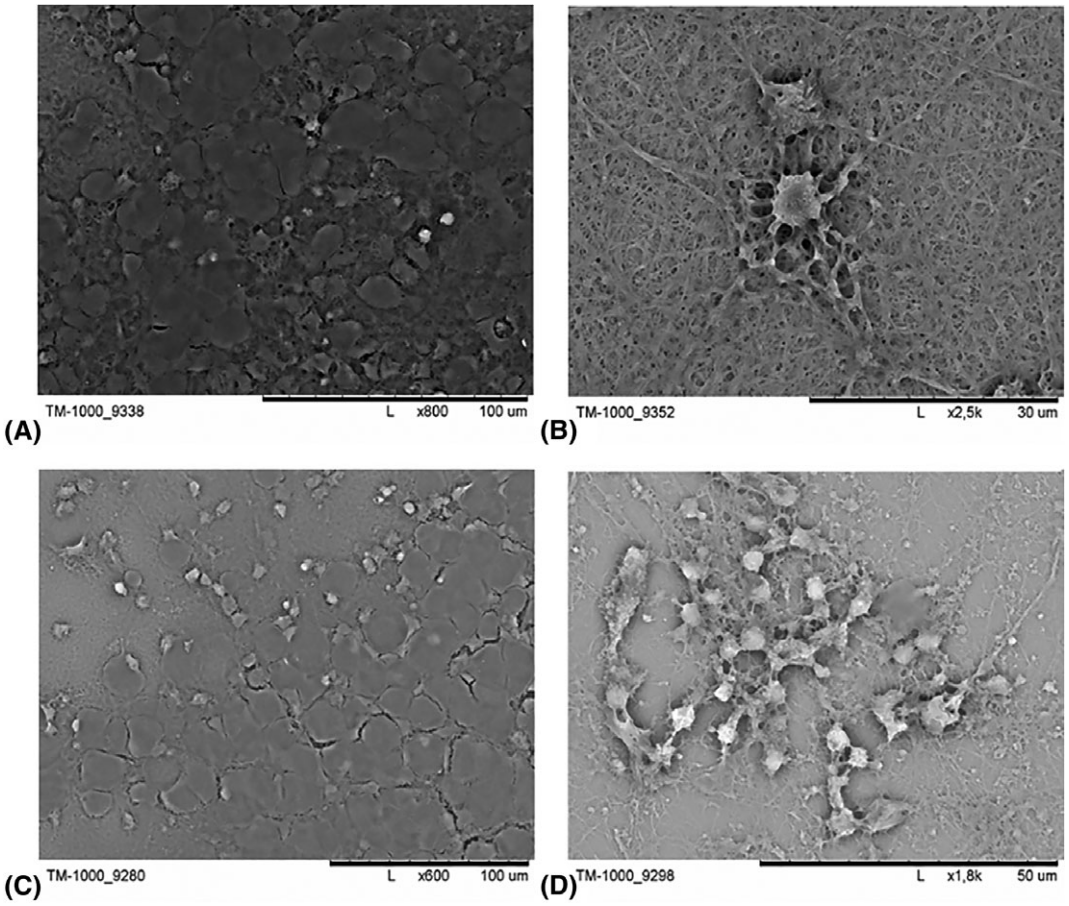

FIGURE 4. Scanning electron microscopy (SEM) pictures of cultured cells immobilized within a polyethyleneimine/chitosan (A, B), polyethyleneimine with fullerenol/chitosan (C, D), alginate/chitosan (E, F), alginate/poly-L-lysine (G, H) scaffold after 2 weeks of culture. Magnification: (A) ×800; (B) ×2500; (C) ×600; (D) ×1800; (E) ×1000; (F) ×2500; (G) ×800; (H) ×2500.

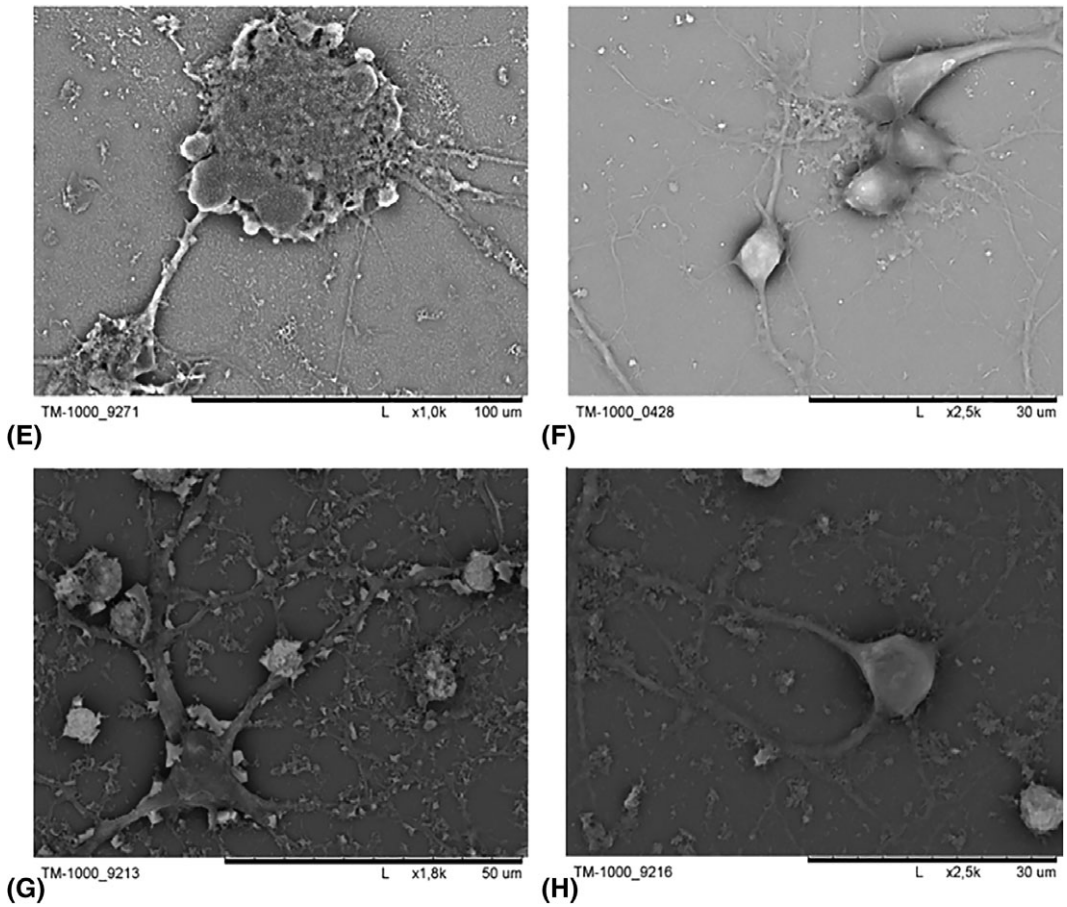

FIGURE 4. (Continued)

Design of a membrane with a negatively charged potential Zeta in the basal layer, with low adhesion between layers

The build-up of ALG/CHIT multilayers, which contain strong polyanions and polycations, involves electrostatic interactions between layers with a negative potential in the basal scaffold layer (-37.60 ± 2.19 mV), with an opposite potential at the layer interface as compared to the basal layer (27.44 ± 2.66 mV).

The morphology of the ALG/CHIT scaffold allows for unusual aggregates of cells adhering to the surface.

Design of a membrane with a negatively-charged potential Zeta in the basal layer, with moderate adhesion between layers.

The build-up of ALG/PLL multilayers, with strong polyanions and weak polycations, involves electrostatic interactions between layers building with a negative potential in the basal layer (-37.60 ± 2.19 mV), and potential at the layer interface close to 0.

Immunofluorescence techniques were used to distinguish cultured cells (from three independent cultures) within the scaffolds. PEI/PLL, PEI + FUOL/PLL, and PEI + FUOL/CHIT layers supported mainly astrocyte growth (Fig. 5). We noted light green fluorescence indicating the presence of cells containing glial fibrillary protein in all samples of these scaffolds. Damaged neurons were also observed in PEI/PLL scaffolds [Fig. 5(C)].

Then we investigated cell growth on the PEI/CHIT, ALG/CHIT, and ALG/PLL scaffolds. As a control we applied poly-D-lysine/laminin (PDL/LAM) coating of the culture wells [Fig. 6(D)]. Green fluorescence indicating the neuronal skeleton (MAP2) was observed in all examined samples. However, some astrocytes, stained in red, were also found within the evaluated scaffolds [Fig. 6(A,B)]. Astrocytes were observed in a minority of ALG/PLL scaffolds [Fig. 6(C)] similarly as observed for PDL/LAM [Fig. 6(D)]. Although it seems that more growing neurons are observed on the ALG/CHIT scaffold.

Western blot analysis

We next sought to determine whether our immunostaining results indicating the presence of MAP2 and GFAP could be confirmed by analyzing protein levels in cultured cells grown on different membranes. To achieve this goal, we separated total protein extracts of cultured cells by sodium-dodecyl sulfate-polyacrylamide gel electrophoresis (SDS-PAGE) and performed immunoblotting (Fig. 7). Western blot analysis revealed that the highest level of the neuronal marker MAP2 was detected in cells grown on ALG/CHIT membranes and PDL/Laminin (PDL/LAM; control). Densitometric analysis

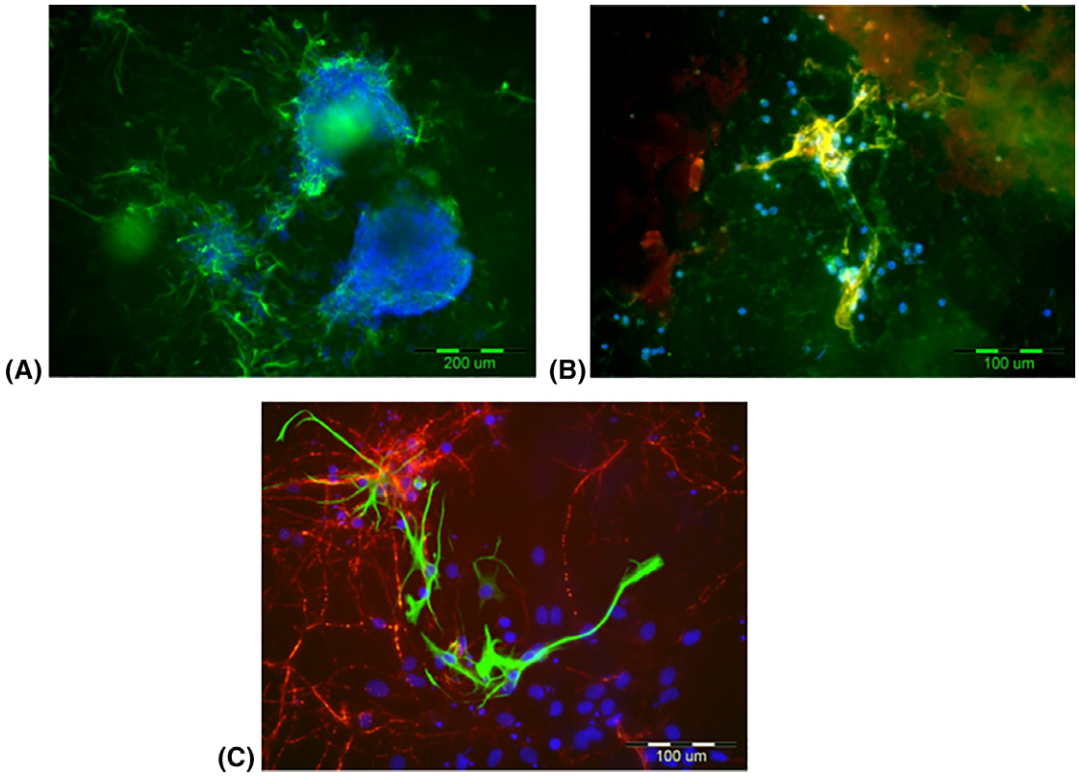

FIGURE 5. Visualization of cultured cells immobilized within polyethyleneimine with fullerenol/chitosan (A), polyethyleneimine with fullerenol/poly-L-lysine (B), polyethyleneimine/poly-L-lysine (C) membrane scaffolds after 2 weeks of culture. The light green fluorescence shows astrocytes. The red fluorescence shows neurons. Nuclei of cells are stained in blue.

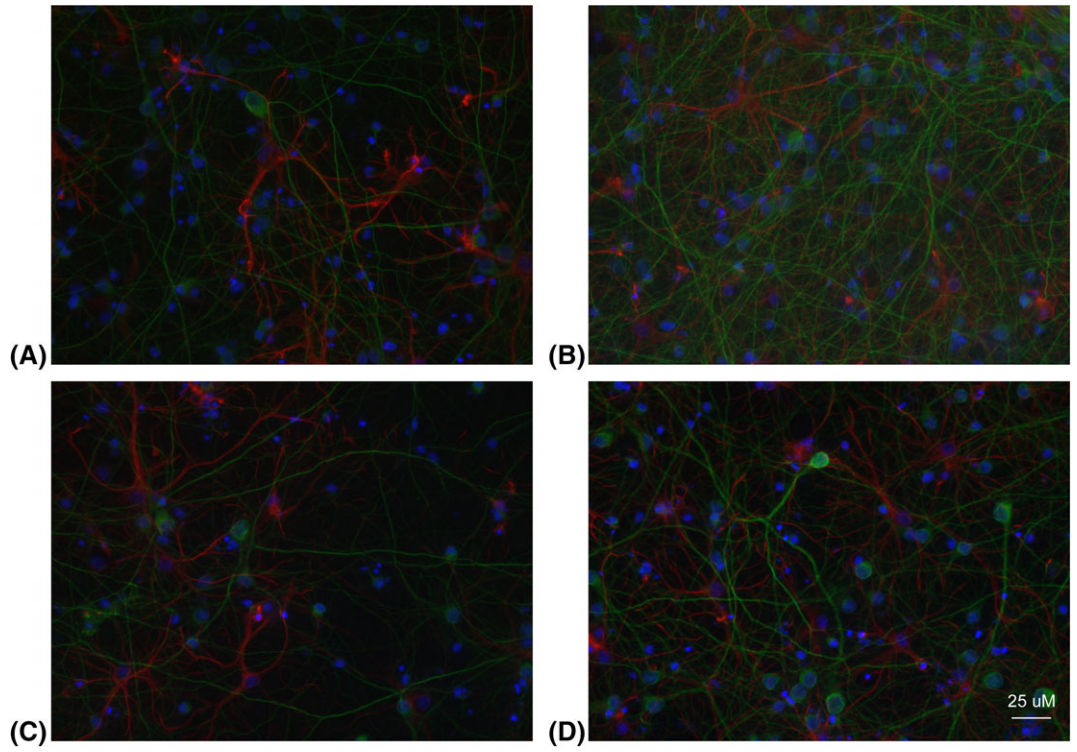

FIGURE 6. Visualization of cultured cells immobilized within polyethyleneimine/chitosan (A), alginate/chitosan (B), alginate/poly-L-lysine (C) membrane scaffolds and on poly-D-lysine/laminin (D) covering after 2 weeks of culture. Light green fluorescence indicates neurons. Red fluorescence indicates the presence of astrocytes. Cell nuclei are shown in blue.

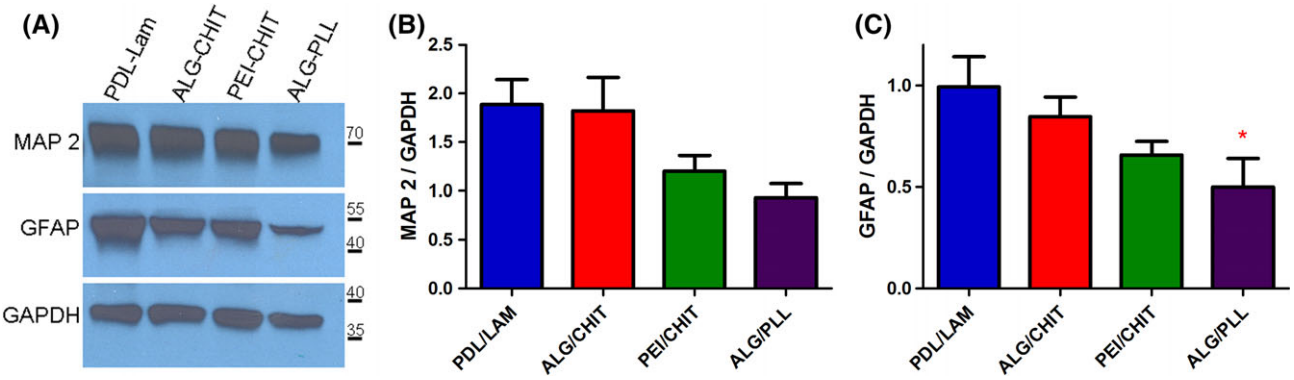

FIGURE 7. (A) MAP2 and GFAP expression in whole-cell cortical lysates from neuronal cultures grown on poly-D-lysine/laminin covering, and on alginate/chitosan, polyethyleneimine/chitosan and alginate/poly-L-lysine scaffolds. GAPDH was used as a loading control. The molecular masses of the markers that were run on same gel are shown on the right. Bars indicate protein band quantitation, showing MAP2 (B) and GFAP (C) levels normalized to that of GAPDH. Each assay was performed six times using six independent cultures. $*p < 0.05$ (one-way ANOVA).

revealed MAP2/GAPDH ratio values (Fig. 7) of 1.82 for ALG/CHIT, 1.20 for PEI/CHIT, 0.93 for ALG/PLL and approximately 1.88 for PDL/LAM membranes [Fig. 7(B)]. No significant differences were detected between control and other membranes ($p > 0.05$). Astrocyte marker (GFAP) levels [Fig. 7(C)], expressed by the GFAP/GAPDH ratio, were approximately two-fold lower than MAP2/GAPDH levels for all evaluated membranes, with the lowest level of astrocytes observed for ALG/PLL membranes ($*p < 0.05$). GFAP/GAPDH values were 0.85 for ALG/CHIT, 0.66 for PEI/CHIT, 0.50 for ALG/PLL, and 0.99 for PDL/LAM membranes. These data point to higher levels of neurons and astrocytes in cells growing on PDL/LAM and ALG/CHIT than on PEI/CHIT and ALG/PLL. We report that there are more neurons than astrocytes in cultures grown on all studied membranes, thus confirming our immunofluorescence data [Fig. 6(A–D)].

Gene expression in rat primary cortical neurons cultured on PE scaffolds

We next used gene expression analysis to validate protein expression results. Cells were cultured on glass coverslips covered by ALG/CHIT, PEI/CHIT and ALG/PLL PE scaffolds up to day 15 *in vitro* (DIV15). As a control, rat primary cortical neurons cultured on glass coverslips covered by PDL/Laminin (DIV15) were used. The presence of neurons and astrocytes in rat primary cortical neuron cultures growing on PE scaffolds was confirmed by immunofluorescence data.

FAM dye-labeled TaqMan probes were used to estimate the relative mRNA levels of genes that encode neuronal and astrocyte markers in rat primary cortical neurons cultured on PE scaffolds. Neuron markers included *Rbfox3/NeuN* (RNA binding protein FOX-1 homolog 3/Neuronal nuclei), *Map2* (Microtubule-associated protein 2), *Eno2* (Enolase 2); the GABAergic interneuron marker used was *Calb2* (Calretinin); and astrocyte markers included *Gfap* (Glial fibrillary acidic protein) and S100b (S100 calcium-binding protein B). All markers were normalized to the endogenous control gene *Gapdh.*

Rbfox3/NeuN, Map2, and *Calb2* neuronal marker expression levels in rat primary cortical neurons cultured on glass coverslips covered by PE scaffolds consisting of ALG/CHIT, PEI/CHIT, and ALG/PLL was approximately five-fold lower than in neurons cultured on PDL/Laminin ($p < **$ or $p < *$). The highest expression of neuronal markers among PE scaffolds was observed in cultures growing on ALG/PLL [Fig. 8(A,B,D)]. The expression of the neuronal marker *Eno2* was reduced three-fold in cells grown on ALG/CHIT and PEI/CHIT scaffolds ($p < *$) as compared to PDL/Laminin; however, there was no statistical difference between ALG/PLL and the control [Fig. 8(C)]. The expression level of the astrocyte marker *S100b* in rat primary cortical neurons cultured on glass coverslips covered by ALG/PLL was approximately five-fold lower than in neurons cultured on PDL/Laminin, while it was 20-fold lower on ALG/CHIT and PEI/CHIT scaffolds [$p < **$; Fig. 8(E)]. The expression of the astrocyte marker *Gfap* was reduced three-fold in cells grown on ALG/CHIT and PEI/CHIT scaffolds ($p < *$), but it was similar to that of the control in cells grown on ALG/PLL [Fig. 8(F)]. These data show the highest levels of neuronal and astrocyte markers in cells grown on ALG/PLL among all analyzed PE scaffolds.

DISCUSSION

Some groups of scaffold designs, differing in the charge of basic layer and the strength of applied PEs, were analyzed in the present study. The scaffolds constructed of the bilayer with negatively charged basic layer built of weak PE or weak and strong PE as well as the scaffolds constructed of the bilayer with positively charged basic layer built of strong PE or weak and strong PE. The materials applied to scaffold construction are all regarded as bioresorbable or biodegradable. The applied membrane cut-off was 150 kDa, sufficient for nutrient and metabolite transport as well as brain delivery.

The applied membranes as ALG/CHIT, ALG/PLL, PEI/CHIT offer surfaces allowing for reproducibly-good neurite outgrowth as identified by immunostaining to MAP2. Cell survival in culture on these scaffolds lasts for at least 2 weeks what is confirmed by immunocytochemistry, protein expression and RT-PCR data. However, there were some discrepancies between microscopic (SEM) visualization and

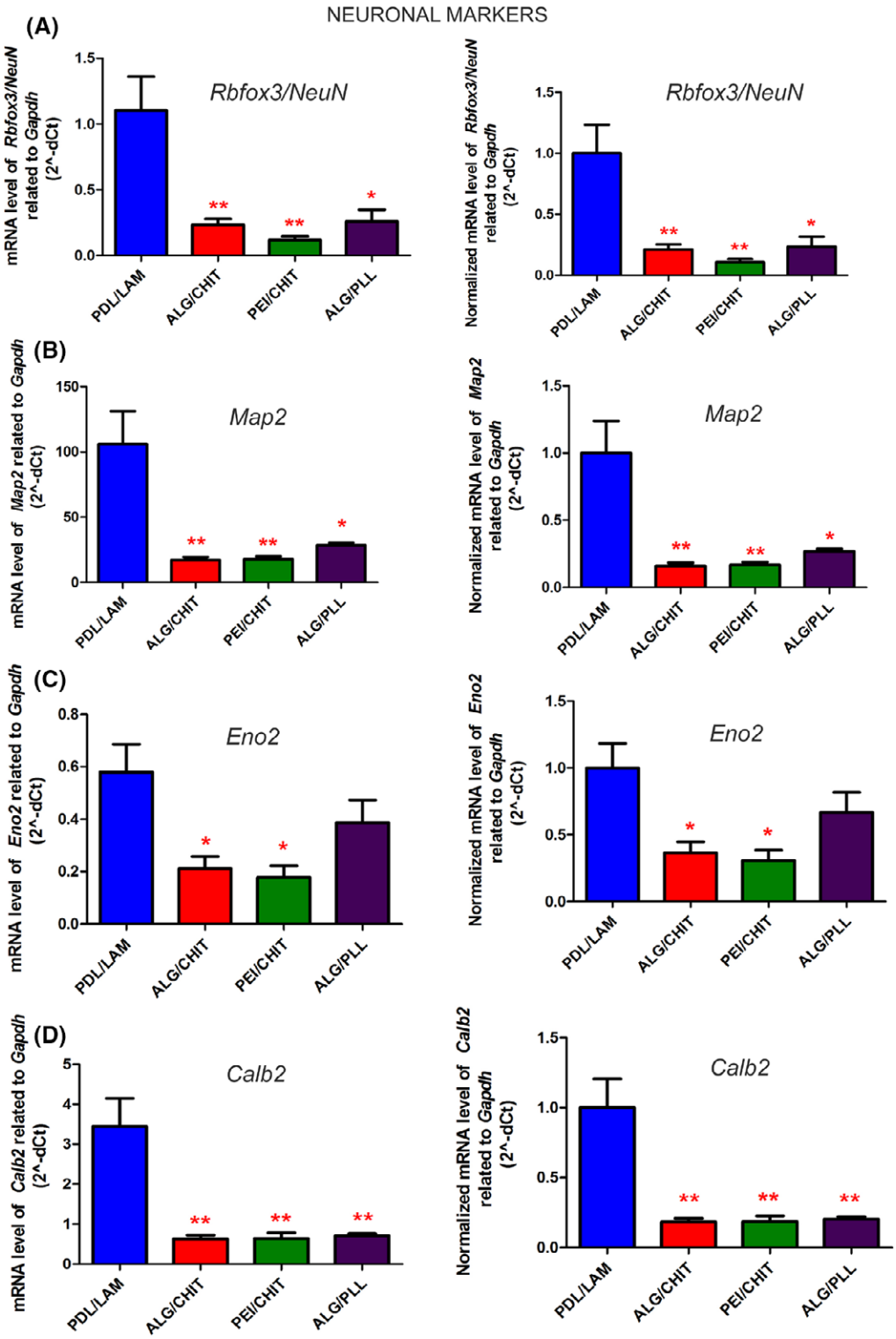

FIGURE 8. Gene expression analysis in rat primary cortical neurons cultured on polyelectrolyte scaffolds. mRNA levels of neuronal markers (A – *Rbfox3/NeuN*; B – *Map2*; C – *Eno2*; D – *Calb2*) and astrocyte markers (E – *S100b* i F – *Gfap*) in rat primary cortical neurons cultured on alginate/-chitosan, polyethyleneimine/chitosan and alginate/poly-L-lysine scaffolds was compared to control primary cortical neurons from rat primary cortical neurons cultured on PDL/Laminin using qRT-PCR. Gene expression results were normalized to *Gapdh.* Data from primary cortical neurons cultured on PDL/Laminin were normalized to a value of 1 (plots on the right part of the figure). Statistically significant gene expression changes are shown (*$p < 0.05$, **$p < 0.005$, and ***$p < 0.0005$). Graphical results represent data from three independent mRNA preparations.

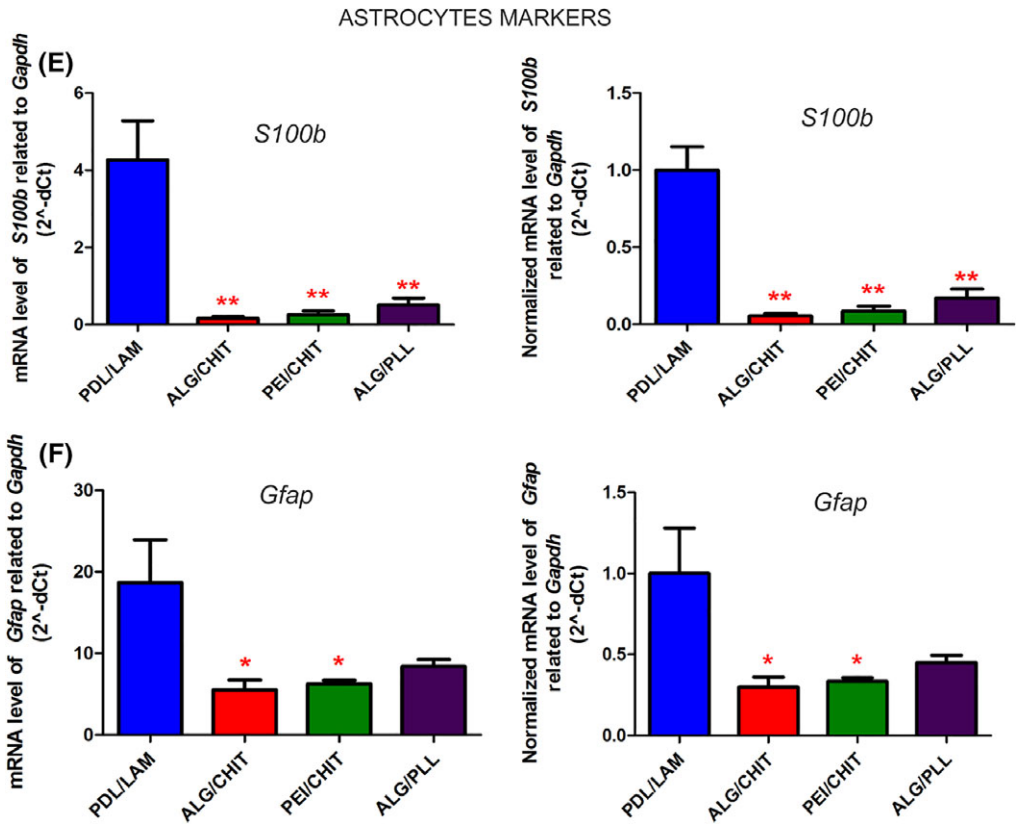

FIGURE 8. (Continued)

protein expression results regarding ALG/CHIT membranes: *via* SEM, we observed adherent aggregates of cells on the membrane surface. We applied some configurations involving materials modified with hydroxylated fullerene to build scaffolds. The water-soluble, hydroxylated fullerene has several clinical applications, including use as a drug carrier to bypass blood ocular barriers,[31] also has been demonstrated to prevent NO-induced cytoskeletal depolymerization and nuclear damage, and to accelerate endothelial cell repair.[32,33] Moreover, neuroprotective activity of water-soluble fullerene derivatives has been reported;[34] nevertheless, we found that it was not able to enhance neuronal growth.

The membrane materials chosen to build a given scaffold should exhibit multiple properties to support neuronal cell growth. First, a scaffold must enable nutrient and metabolite transport to the settled cells. Furthermore, the scaffold should influence neuronal cell differentiation and growth, and act as an anti-bacterial support. These properties are crucial for the potential of membrane scaffold applications for surgical wound healing. Such a material can act as a barrier to scar growth in the spinal canal. Moreover, it could support nerve cell growth in the context of neuronal deficiency diseases.

Concluding, among scaffold properties enhancing neuronal cell growth, we found that neither the basic layer charge, the type of PE (weak, strong), nor adhesion work between layers influenced cell growth. Microscopic analysis of PEI/CHIT, ALG/CHIT, ALG/PLL scaffolds demonstrated that they support neuronal growth. In particular, we observed fewer astrocytes, which are potentially inconvenient for neural regeneration, in cells cultured on ALG/PLL scaffolds. On the other hand, the neuron to astrocyte ratio was comparable for ALG/CHIT, ALG/PLL, and PEI/CHIT scaffolds *via* western blot results. PEI/CHIT, ALG/CHIT, ALG/PLL layers promote growth of neurons, that express dendritic marker MAP2, over astrocytes and other glia which in turn deliver growth factors, hormones and amino acids to neurons.

The mRNA expression level of *Map2* was higher for cells grown on ALG/PLL, and we observed demonstrable differences compared to cells grown on ALG/CHIT and PEI/CHIT. It is notable that ALG/PLL showed strong N–H interactions between scaffold layers.

CONCLUSIONS

We conclude that the potential value in the interface between layers most strongly influences cell growth; however, the influence of N–H interactions cannot be excluded. Thus, we recommend ALG/PLL scaffolds for nerve growth applications. Obtained results indicate the capability of chosen scaffolds allowing survival of neurons in culture for over 2 weeks in controllable regeneration of neural networks in nanomedicine.

ACKNOWLEDGMENTS

This work was partly supported by funds from the National Science Centre in Poland [DEC-2011/01/D/NZ3/02051] to JG-B and the National Science Centre in Poland [Grant no. 2014/15/D/NZ3/05181 to MCZ].

REFERENCES

1. Reubinoff BE, Itsykson P, Turetsky T, Pera MF, Reinhartz E, Itzik A, Ben-Hur T. Neural progenitors from human embryonic stem cells. Nat Biotechnol 2001;19(12):1134–1140.
2. Cao Q-L, Zhang YP, Howard RM, Walters WM, Tsoulfas P, Whittemore SR. Pluripotent stem cells engrafted into the normal or lesioned adult rat spinal cord are restricted to a glial lineage. Exp Neurol 2001;167(1):48–58.
3. Lee I-C, Wu Y-C. Facilitating neural stem/progenitor cell niche calibration for neural lineage differentiation by polyelectrolyte multilayer films. Colloids Surf B Biointerfaces 2014;121:54–65.
4. Zhou K, Sun GZ, Bernard CC, Thouas GA, Nisbet DR, Forsythe JS. Optimizing interfacial features to regulate neural progenitor cells using polyelectrolyte multilayers and brain derived neurotrophic factor. Biointerphases 2011;6(4):189–199.
5. Vodouhê C, Schmittbuhl M, Boulmedais F, Bagnard D, Vautier D, Schaaf P, Egles C, Voegel JC, Ogier J. Effect of functionalization of multilayered polyelectrolyte films on motoneuron growth. Biomaterials 2005;26(5):545–554.
6. Ryu S, Kim B-S. Culture of neural cells and stem cells on graphene. Tissue Eng Regenerat Med 2013;10(2):39–46.
7. Liu HW, Huang WC, Chiang CS, Hu SH, Liao CH, Chen YY, Chen SY. Arrayed rGOSH/PMASH microcapsule platform integrating surface topography, chemical cues, and electrical stimulation for three-dimensional neuron-like cell growth and neurite sprouting. Adv Funct Mater 2014;24(24):3715–3724.
8. Pavlukhina S, Sukhishvili S. Polymer assemblies for controlled delivery of bioactive molecules from surfaces. Adv Drug Deliv Rev 2011;63(9):822–836.
9. Teramura Y, Kaneda Y, Iwata H. Islet-encapsulation in ultra-thin layer-by-layer membranes of poly (vinyl alcohol) anchored to poly (ethylene glycol)–lipids in the cell membrane. Biomaterials 2007; 28(32):4818–4825.
10. Sun J, Huang Y, Shi Q, Chen X, Jing X. Oxygen carrier based on hemoglobin/poly (L-lysine)-block-poly (L-phenylalanine) vesicles. Langmuir 2009;25(24):13726–13729.
11. Schanze KS, Shelton AH. Functional polyelectrolytes. Langmuir 2009;25(24):13698–13702.
12. Wong JE, Zastrow H, Jaeger W, Von Klitzing R. Specific ion versus electrostatic effects on the construction of polyelectrolyte multilayers. Langmuir 2009;25(24):14061–14070.
13. Cui H, Shao J, Wang Y, Zhang P, Chen X, Wei Y. PLA-PEG-PLA and its electroactive tetraaniline copolymer as multi-interactive injectable hydrogels for tissue engineering. Biomacromolecules 2013; 14(6):1904–1912.
14. Borkowska M, Godlewska E, Antosiak-Iwańska M, Kinasiewicz J, Strawski M, Szklarczyk M, Granicka LH. Suitability of polyelectrolyte shells modified with fullerene derivate for immunoisolation of cells. Experimental study. J Biomed Nanotechnol 2012;8(6):912–917.
15. Iler R. Multilayers of colloidal particles. J Colloid Interface Sci 1966; 21(6):569–594.
16. Clark SL, Hammond PT. The role of secondary interactions in selective electrostatic multilayer deposition. Langmuir 2000;16(26): 10206–10214.
17. Fu Y, Bai S, Cui S, Qiu D, Wang Z, Zhang X. Hydrogen-bonding-directed layer-by-layer multilayer assembly: Reconformation yielding microporous films. Macromolecules 2002;35(25): 9451–9458.
18. Kharlampieva E, Kozlovskaya V, Tyutina J, Sukhishvili SA. Hydrogen-bonded multilayers of thermoresponsive polymers. Macromolecules 2005;38(25):10523–10531.
19. Teramura Y, Iwata H. Cell surface modification with polymers for biomedical studies. Soft Matter 2010;6(6):1081–1091.
20. Kotov N. Layer-by-layer self-assembly: The contribution of hydrophobic interactions. Nanostruct Mater 1999;12(5–8):789–796.
21. Martín-López E, Alonso FR, Nieto-Díaz M, Nieto-Sampedro M. Chitosan, gelatin and poly (L-lysine) polyelectrolyte-based scaffolds and films for neural tissue engineering. J Biomater Sci Polym Ed 2012;23(1–4):207–232.
22. Chanda S, Hirst E, Percival E, Ross A. 338. The structure of alginic acid. Part II. J Chem Soc (Resumed) 1952;1833–1837.
23. Kinasiewicz A, Gautier A, Lewińska D, Śmietanka A, Legallais C, Weryński A. Three-dimensional growth of human hepatoma C3A cells within alginate beads for fluidized bioartificial liver. Int J Artif Organs 2008;31(4):340–347.
24. Bhatia SR, Khattak SF, Roberts SC. Polyelectrolytes for cell encapsulation. Curr Opin Colloid Interface Sci 2005;10(1–2):45–51.
25. Boussif O, Lezoualc'h F, Zanta MA, Mergny MD, Scherman D, Demeneix B, Behr JP. A versatile vector for gene and oligonucleotide transfer into cells in culture and in vivo: Polyethylenimine. Proc Natl Acad Sci USA 1995;92(16):7297–7301.
26. Gruszczynska-Biegala J, Kuznicki J. Native STIM2 and ORAI1 proteins form a calcium-sensitive and thapsigargin-insensitive complex in cortical neurons. J Neurochem 2013;126(6):727–738.
27. Gruszczynska-Biegala J, Sladowska M, Kuznicki J. AMPA receptors are involved in store-operated calcium entry and interact with STIM proteins in rat primary cortical neurons. Front Cell Neurosci 2016; 10(251).
28. Czeredys M, Gruszczyńska-Biegała J, Schacht T, Methner A, Kuznicki J. Expression of genes encoding the calcium signalosome in cellular and transgenic models of Huntington's disease. Front Mol Neurosci 2013;6(42).
29. Granicka L, Antosiak-Iwańska M, Godlewska E, Hoser G, Strawski M, Szklarczyk M, Dudziński K. The experimental study of polyelectrolyte coatings suitability for encapsulation of cells. Artif Cells Blood Substit Biotechnol 2009;37(5):187–194.
30. Granicka L, Borkowska M, Grzeczkowicz A, Stachowiak R, Szklarczyk M, Bielecki J, Strawski M. The targeting nanothin polyelectrolyte shells in system with immobilized bacterial cells for antitumor factor production. J Biomed Mater Res A 2014;102(8):2662–2668.
31. Roberts JE, Wielgus AR, Boyes WK, Andley U, Chignell CF. Phototoxicity and cytotoxicity of fullerol in human lens epithelial cells. Toxicol Appl Pharmacol 2008;228(1):49–58.
32. Lao F, Li W, Han D, Qu Y, Liu Y, Zhao Y, Chen C. Fullerene derivatives protect endothelial cells against NO-induced damage. Nanotechnology 2009;20(22):225103.
33. Isakovic A, Markovic Z, Todorovic-Markovic B, Nikolic N, Vranjes-Djuric S, Mirkovic M, Dramicanin M, Harhaji L, Raicevic N, Nikolic Z, Trajkovic V. Distinct cytotoxic mechanisms of pristine versus hydroxylated fullerene. Toxicol Sci 2006;91(1):173–183.
34. Kotelnikova R, Smolina A, Grigoryev V, Faingold I, Mischenko DV, Rybkin AY, Poletayeva DA, Vankin GI, Zamoyskiy VL, Voronov II, Troshin PA, Kotelnikova AI, Bachurinb SO. Influence of water-soluble derivatives of [60] fullerene on therapeutically important targets related to neurodegenerative diseases. MedChemComm 2014;5(11):1664–1668.